Study the Synergistic Inhibition for Nanocomposite Based on Biosynthesized Iron Nanoparticle and Purine Compounds on Steel Corrosion in Sulfuric Acid

Ahmed A. Farag[1], W. Ahmed[2], Khaled Zakaria[3], Ibrahim M. Nassar[4]

[1,2,3,4] Egyptian Petroleum Research Institute (EPRI), 1 Ahmed El-Zomor St., Nasr City, 11727, Cairo, Egypt

Abstract: ***Nanocomposite material based on Iron nanoparticles colloidal (Fe–NPC) and Purine were used through this work. (Fe–NPC) was biosynthesized and characterized by dynamic light scattering (DLS) and UV-visible spectroscopy. Fe–NPC was evaluated as synergistic inhibition with two purine inhibitors namely 1H-pyrazolo[3,4-d]pyrimidin-4(2H)-one (PU1) and 6-[(1-methyl-4-nitro-5-imidazolyl) sulfanyl] purine (PU2) on the corrosion of carbon steel in 0.5 mol dm^{-3} H_2SO_4 solution by electrochemical techniques. The potentidynamic polarization curves indicated that PU1 and PU2 behave as a mixed-type inhibitor while in the presence of Fe–NPC and its mixture with PU1 and PU2 behave as a cathodic inhibitor. There is a synergism between purine inhibitors and the biosynthesis Fe–NPC, and the values of synergism parameter (S) are higher than unity.***

Keywords: Metals, Nanostructures, Organic compounds, electrochemical techniques, and Corrosion

1. Introduction

Nanotechnology has attracted a great interest in recent years due to its expected impact on many areas such as energy, catalysis and medicine. Nanoparticles have been synthesized by various physical and chemical processes. However, some chemical methods cannot avoid the use of toxic chemicals in the synthesis process [1, 2].

Eco-friendly biosynthesis of nanoparticles (NP) are accomplished using microorganism which grabs target ions from their solutions, and then accumulates the reduced metal in its element form through enzymes generated by microbial cell activities [3,4]. Among microorganisms, Fungi are more advantageous since they fast grow, easy to handle and easy for fabrication [5]. Fungi are regarded as the organisms that produce nanoparticles because of their enormous secretor components, which involve in the reduction and capping of nanoparticles [6].

A Fusarium oxysporum fungus is the only fungus, which has been completely explored and exploited to the maximum for the production of various nanoparticles [7–14]. It extracellular synthesized various nanoparticles like gold, silver, bimetallic Au–Ag alloy, silica, titanium, quantum dots and strontianite, Bi_2O_3. With the mixture of salts K_3 [Fe $(CN)_6$] and K_4 [Fe $(CN)_6$] After 24 h, it produced crystalline quasi-spherical with 20–50 Nm in size magnetite nanoparticles and single-domain characteristics.

Acid solutions are widely used in the industry, some of the important fields of application being acid pickling of iron and steel, chemical cleaning and processing, ore production and oil well acidification [15−19]. Because of the general aggression of acid solutions, inhibitors are commonly used to reduce the corrosive attack on metallic materials. Most well-known acid inhibitors are organic compounds containing nitrogen, sulfur, and oxygen atoms. Among them, nitrogen containing heterocyclic compounds is considered to be effective corrosion inhibitors for steel in acid media [20]. N-heterocyclic compound inhibitors act by adsorption on the metal surface, and the adsorption of N-heterocyclic inhibitor takes place through nitrogen heteroatom, as well as those with triple or conjugated double bonds or aromatic rings in their molecular structures. Although N-heterocyclic organic compounds have good anti-corrosive activity; they are highly toxic to both human beings and the environment [21].

The safety and environmental issues of corrosion inhibitors arisen in industries has always been a global concern. These toxic effects have led to the use of eco-friendly and harmless N-heterocyclic compounds as inhibitors. As an important N-heterocyclic compound, purine and purine derivatives are non-toxic and biodegradable; this makes the investigation of their inhibiting properties significant within the context of the current priority to produce eco-friendly inhibitors [22].

In order to improve the inhibiting force, synergistic inhibition effect (synergism) is an effective method [23]. Synergistic inhibition is an effective means to improve the inhibiting force of the inhibitor, to decrease the amount of usage and to diversify the application of the inhibitor in acidic media. It is necessary for corrosion scientists to discover, explore and use synergism in the complicated corrosive media. The aim of this work is to study the inhibition efficiency of purine derivatives namely, 1H-pyrazolo[3,4-d]pyrimidin-4(2H)-one (PU1) and 6-[(1-methyl-4-nitro-5-imidazolyl)sulfanyl]purine (PU2) as the corrosion inhibitor for carbon steel in 0.5 mol dm^{-3} H_2SO_4 using potentiodynamic polarization and electrochemical impedance spectroscopy (EIS) techniques, hence improve their efficiency synergistically by the biosynthesis Fe–NPC.

2. Experimental

2.1. Biosynthesis of iron nanoparticles colloids (Fe–NPC)

2.1.1. Organism, culture maintenance and biomass preparation

The Fusarium oxysporum fungus was obtained from the MERCEN, Cairo, Egypt. The biomass were prepared as follows; the fungus was grown aerobically in MGYP media containing 1% glucose (w/v) as a carbon source, 0.3% yeast extract, 0.3% malt extract and 0.5% peptone. The pH was then adjusted to 6.5 with 0.5 mol dm^{-3} HCl. The medium was inoculated and incubated on an incubating shaker at 301 K and 200 rpm for 96 h. Later on, the biomass was harvested, followed by extensive washing with distilled water.

2.1.2. Iron nanoparticles

The nanoparticles were prepared according to the reference [24]. The iron nanoparticles (Fe–NP) were typically prepared as following; after the biomass prepared, a 30 ml of the pre-culture was transferred to 150 ml of a medium consisting of 10 g dm^{-3} glucose, 14.2 g dm^{-3} Sodium nitrate and 1 mol dm^{-3} trace element solution in 500 ml Erlenmeyer flasks followed by incubation at 225 rpm and 301 K. The solution was then filtered with filter paper (0.45 µm pore size). The cell filtrate was mixed with a 1 mol dm^{-3} Fe $(NO_3)_3$ solutions (1:1 ratio) and agitated at 301 K for 72 h, and finally obtained iron nanoparticles colloids (Fe–NPC).

2.2. Carbon steel composition

Tests were performed on carbon steel of the following composition (wt. %): 0.07% C, 0.24% Si, 1.35% Mn, 0.017% P, 0.005% S, 0.16% Cr, 0.18% Ni, 0.12% Mo, 0.01% Cu and the remainder Fe.

2.3. Corrosive medium

The aggressive solution was prepared by dilution of analytical grade, 98% H_2SO_4 with distilled water to produce 0.5 mole dm^{-3} H_2SO_4. The corrosion tests were performed in 0.5 mol dm^{-3} H_2SO_4 in the absence and presence of various concentrations of inhibitors. The inhibitors solutions were prepared in 0.5 mol dm^{-3} H_2SO_4. For each experiment, a freshly prepared solution was used under air atmosphere without stirring at 298 K.

2.4. Electrochemical measurements

The electrochemical measurements were carried out using Volta lab 40 (Tacussel-Radiometer PGZ301) potentiostate and controlled by Tacussel corrosion analysis software model (Voltamaster 4) at under static condition. The corrosion cell used had three electrodes. The reference electrode was a saturated calomel electrode (SCE). A platinum electrode was used as auxiliary electrode. Carbon steel coupons having the area of 1 cm^2 were used as a working electrode. The working electrode was immersed in test solutions for 30 minutes to a establish steady state open circuit potential (E_{ocp}). After measuring the E_{ocp}, the electrochemical measurements were performed. The EIS experiments were conducted in the frequency range with high limit of 10^5 Hz and different low limit 10^{-2} Hz at open circuit potential. The polarization curves were obtained in the potential range from −900 to −200 mV (SCE) with 1 mV s^{-1} scan rate. To achieve a reproducibility three parallel experiments were performed for each test.

2.5. UV–visible measurement

The absorbance spectrum of Fe–NPC was scanned in the range of 200–800 nm using a UV–visible spectrophotometer (JASCO, V570, and USA).

2.6. Dynamic light scattering (DLS)

The DLS technique was used to determine the prepared particle size. For a measurement, the Fe–NPC was subjected to ultra-sonication for 10 min at a power level of 6 and a duty cycle of 70%. After sonication, 3 ml nanoparticles colloids were then transferred to the zeta seizer apparatus (Nano-ZS, Malvern Instrument, UK). The particle size was measured three times for each sample at 633 nm wavelength corresponding to He-Ne laser.

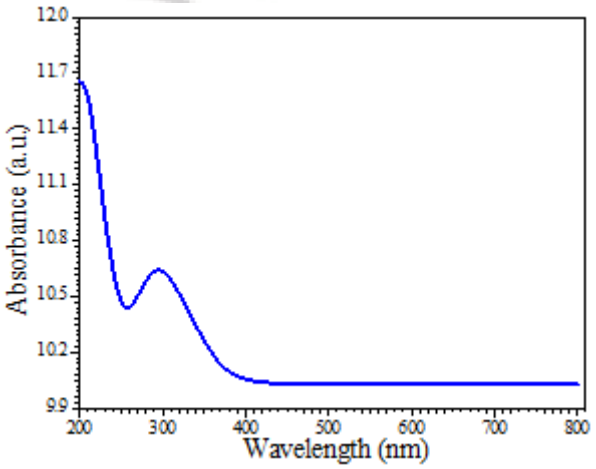

Figure 1: UV-Visible absorption spectrum recorded from the reaction medium Fe–NPC after 72 h commencement of the reaction

3. Results and Discussion

3.1. Characterization of the biosynthesized Fe–NPC

3.1.1. UV-visible absorption

The UV-visible absorption spectrum at 200–800 nm in aqueous medium of Fe–NPC after 72 h reaction time is displayed in Fig. 1. The Absorption band observed at 270 nm was attributed to the electronic excitations in tryptophan and tyrosine residues in the proteins [25]. Meanwhile, the other band at 302 nm was assigned to the formation of Fe metal. The good symmetric absorption peak implies that the size distribution of the nanoparticles is narrow. This observation indicated the release of proteins into solution by fusarium oxysporum fungus and hence the nanoparticles produced.

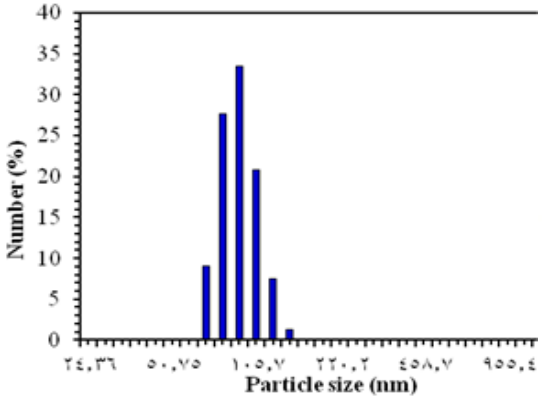

Figure 2: The particle size and particle size distribution for the prepared Fe–NPC measured by DLS technique.

3.1.2. Dynamic light scattering (DLS)

Fig. 2 shows the results from the DLS to determine the particle size and particle size distribution of the Fe metal. It revealed that the formed materials are nanoscale and had the mean particle size of 91 nm. Fig. 2 also showed the particle size distribution along the synthesized particles.

3.2. Potentiodynamic polarization measurements

The synergistic inhibition for nanocomposite of Fe–NPC and purine inhibitors (PU1 and PU2) on the polarization curves of carbon steel in 0.5 mol dm^{-3} H_2SO_4, at 298 K is represented in Fig. 3. The electrochemical parameters such as corrosion potential (E_{corr}), corrosion current density (i_{corr}), cathodic Tafel constant (β_c), anodic Tafel slope (β_a) and inhibition efficiency (η_p) are calculated and given in Table 1. The η_p was calculated from polarization measurements according to the relation given below [26];

$$\eta_p = \left(\frac{i_t - i_t^o}{i_t}\right) \times 100 \quad (1)$$

where i and i° are uninhibited and inhibited corrosion current densities, respectively.

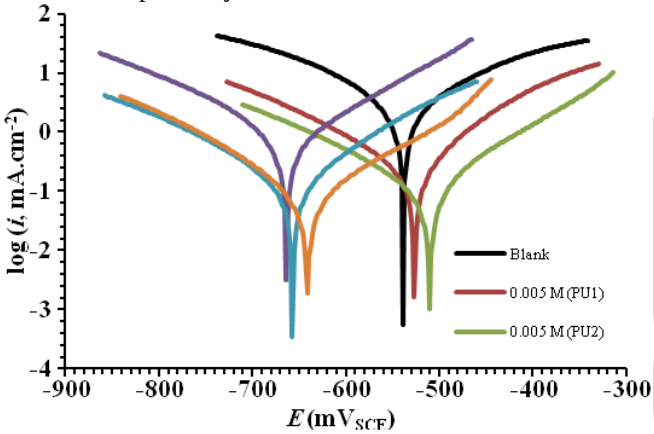

Figure 3: Polarization curves for carbon steel in (0.5 mol dm–3) H2SO4 and containing investigated inhibitors at 298 K.

The polarization curves show that the PU1 and PU2 has an effect on both, the cathodic and anodic slopes (β_c and β_a) and suppressed both cathodic and anodic processes. This indicates a modification of the mechanism of cathodic hydrogen evolution as well as anodic dissolution of iron, which suggest that inhibitor powerfully inhibits the corrosion process of carbon steel. The suppression of cathodic process can be due to the covering of the surface with monolayer due to the adsorbed inhibitor molecules. It can also be seen from Table 1 that the anodic Tafel slope (β_a) decreases in the presence of inhibitors. This observation may be ascribed to changes in the charge transfer coefficient for the anodic dissolution of iron by virtue of the presence of an additional energy barrier due to the presence of adsorbed inhibitor.

According to Riggs [27], the classification of a compound as an anodic or cathodic type inhibitor is feasible when the corrosion potential (E_{corr}) displacement is at least 85 mV. Inspection of Table 1 reveals that E_{corr} values do not show any significant change in the presence of (5×10^{-3} mol dm^{-3}) of the inhibitor suggesting that PU1 and PU2 are mixed-type inhibitor in 0.5 mol dm^{-3} H_2SO_4, which influences both metal dissolution and hydrogen evolution [28].

Table 1: Potentiodynamic polarization parameters for the corrosion of steel in 0.5 mol dm^{-3} H_2SO_4 in the absence and presence of various concentrations of investigated inhibitors at 298 K

Inhibitor	*C (Purine) (mol dm^{-3})*	*C (Fe–NPC) (mol dm^{-3})*	*$-E_{corr}$ (mV_{SCE})*	*i_{corr} (mA cm^{-2})*	*β_a (mV dec^{-1})*	*$-\beta_c$ (mV dec^{-1})*	*θ*	*η_p (%)*
Blank	0	0	538.5	6.1184	248.5	232.9	—	—
PU1	5×10^{-3}	0	526.5	0.5859	109.9	158.1	0.904	90.4
PU2	5×10^{-3}	0	510.5	0.3022	118.7	162.7	0.951	95.1
Fe–NPC	0	1×10^{-3}	663.4	1.0941	148.5	166.1	0.821	82.1
PU1+ Fe–NPC	1×10^{-4}	1×10^{-4}	657.0	0.2900	140.5	174.5	0.953	95.3
PU2 + Fe–NPC	1×10^{-4}	1×10^{-4}	641.0	0.1362	155.2	132.7	0.978	97.8

The better inhibition performance is seen in the case of PU2 ($C_9H_7N_7O_2S$) than PU1 ($C_5H_4N_4O$). The higher inhibition efficiency of PU2 can be explained by the presence of extra imidazole group and sulfur atom in its molecular structure, which considered being active centers of adsorption. The presence of such groups in molecular structure of inhibitor molecule increases electron density on adsorption centers and leading to an easier electron transfer from the functional group to the metal surface, producing greater coordinate bonding and higher inhibition efficiency [29].

For the prepared nanomaterial, fig. 3 shows potentiodynamic polarization curves for carbon steel in 0.5 mol dm^{-3} H_2SO_4 and containing (1×10^{-3} mol dm^{-3}) for individual nanomaterial Fe–NPC and nanocomposite of (1×10^{-4} mol dm^{-3}) Fe–NPC + (1×10^{-4} mol dm^{-3}) purine inhibitors (PU1 and PU2) at 298 K. It is observed that the nanocomposite produce pronounced effects on the corrosion current density and corrosion potential (E_{corr}) compared to those displayed by individual Fe–NPC or purine inhibitors.

According to data of Table 1 reveals that E_{corr} values show significant negative shift in E_{corr} values (−124.9, −118.5 and −102.5) for individual nanomaterial Fe–NPC and nanocomposite, respectively. This suggests that the Fe–NPC and nanocomposite inhibitors in 0.5 mol dm^{-3} H_2SO_4 formed complex precipitated at the cathodic site of the carbon steel surface, and acts as cathodic inhibitors more than anodic. This also indicates a synergistic inhibition effect between

Fe–NPC and purine inhibitors. Further inspection of Table 1, reveals that the corrosion current density decreases substantially, leading to higher inhibition efficiency of (1 × 10^{-4} mol dm^{-3}) Fe–NPC + (1 × 10^{-4} mol dm^{-3}) purine inhibitors (PU1 and PU2) composite, up to 95.3% and 97.8%, compared to 90.4% and 95.1% obtained for individual (5 × 10^{-3} mol dm^{-3}) of PU1 and PU2, respectively. This indicates a synergistic effect between Fe–NPC and purine inhibitors [30].

3.3. Electrochemical impedance spectroscopy (EIS)

Fig. 4 show the Nyquist plots for carbon steel in (0.5 mol dm^{-3}) H_2SO_4 in the absence and presence of PU1 and PU2 and its synergistic with Fe–NPC at 298 K. The impedance diagrams consist of a large capacitive loop at high frequencies followed by a small inductive loop at low frequency values. The high frequency capacitive loop is usually related to the charge transfer of the corrosion process and double layer behavior. On the other hand, the low frequency inductive loop may be attributed to the relaxation process obtained from adsorption species like $FeSO_4$ or inhibitor species on the electrode surface [31]. It might be also attributed to the re-dissolution of the passivated surface at low frequencies [32].

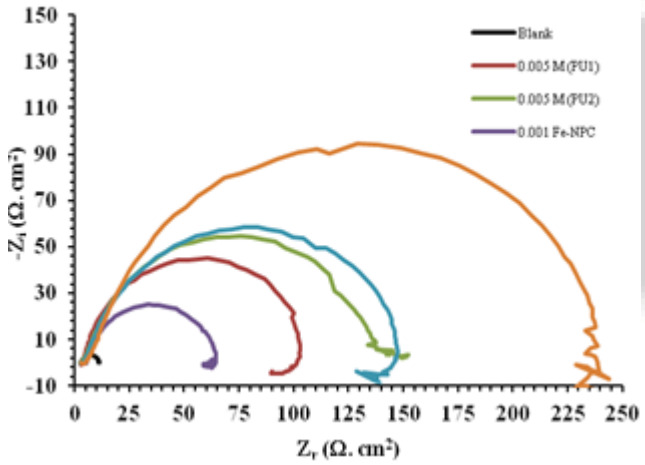

Figure 4: Nyquist plots for carbon steel in (0.5 mol dm–3) H2SO4 and containing investigated inhibitors at 298 K

Furthermore, the diameter of the capacitive loop in the presence of inhibitors is bigger than that in the uninhibited; this indicates that the impedance of carbon steel corrosion increases in the presence of inhibitors. By inspection of Nyquist plots (Fig. 4) also show the capacitive loops are not perfect semicircles which can be attributed to the frequency dispersion effect as a result of the roughness and inhomogeneous of electrode surface [33,34]. The electrochemical parameters derived from Nyquist plots are calculated and listed in Table 2. The values of charge transfer resistance (R_t) were given by subtracting the high frequency impedance from the low frequency one as follows [35]:

$$R_t = Z_{re}(at\ low\ frequency) - Z_{re}(at\ high\ frequency) \quad (2)$$

where ε_0 is the permittivity of space (8.854 × 10-12 Fm-1), ε is the local dielectric constant, d is the thickness of the film and S is the surface area of the electrode. In fact, the decrease in Cdl values can result from a decrease in local dielectric constant and/or an increase in the thickness of the electrical double layer [39, 40].

The impedance diagrams for carbon steel in 0.5 mol dm^{-3} H_2SO_4 containing (1 × 10^{-3} mol dm^{-3}) Fe–NPC and composite of (1 × 10^{-4} mol dm^{-3}) Fe–NPC + (1 × 10^{-4} mol dm^{-3}) purine inhibitors (PU1 and PU2) at 298 K are shown also in Fig. 4. As it is shown in Table 2, the R_t values increase in the presence of Fe–NPC is indicating the inhibition of the corrosion process while the double layer capacitance (C_{dl}) values decrease.

According to data of Table 2, the inhibition efficiency for composite (1 × 10^{-4} mol dm^{-3}) Fe–NPC + (1 × 10^{-4} mol dm^{-3}) purine inhibitors (PU1 and PU2), up to 92.9% and 95.7%, compared to 89.3% and 93.0% obtained for indivdual (5 × 10^{-3} mol dm^{-3}) of PU1 and PU2, respectively. This indicates a synergistic inhibition effect between Fe–NPC and purine inhibitors [41].

The impedance spectra for the Nyquist plots were analyzed by fitting to the equivalent circuit model shown in Fig. 5, which has been used previously to model the steel/acid interface [42]. The circuit comprises a solution resistance R_s shorted by a constant phase element (CPE) that is placed in parallel to the charge transfer resistance R_t.

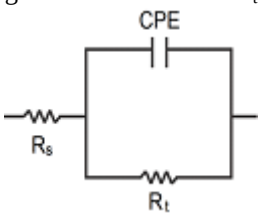

Figure 5: Equivalent circuit model used to fit the impedance data for carbon steel.

Table 2: Impedance electrochemical parameters derived from the Nyquist plots for carbon steel in 0.5 mol dm^{-3} H_2SO_4 in the absence and presence of various concentrations of investigated inhibitors at 298 K

Inhibitor	C (Purine) (mol dm^{-3})	C (Fe–NPC) (mol dm^{-3})	R_s (ohm.cm²)	R_t (ohm.cm²)	C_{dl} (µF cm^{-2})	θ	η_i (%)
Blank	0	0	2.9	9.8	348.5	—	—
PU1	5 × 10^{-3}	0	3.6	91.14	38.4	0.893	89.3
PU2	5 × 10^{-3}	0	3.7	139.9	29.1	0.930	93.0
Fe–NPC	0	1 ×	5.5	57.2	31.2	0.829	82.9
PU1+	1 × 10^{-4}	1 ×	5.6	137.6	18.4	0.929	92.9
PU2 +	1 × 10^{-4}	1 ×	6.9	230.1	15.5	0.957	95.7

The value of the charge transfer resistance is indicative of electron transfer across the interface. The use of the CPE, has been extensively described in the literature [43, 44] and is employed in the model to compensate for the inhomogeneity's in the electrode surface as depicted by the depressed nature of the Nyquist semicircle. The introduction of such a CPE is often used to interpret data for rough solid electrodes. The impedance, Z, of the CPE is [45, 46]:

$$Z_{CPE} = \left[Q(j\omega)^n\right]^{-1} \quad (6)$$

where the coefficient Q is a combination of properties related to different physical phenomena like surface

inhomogeneousness, electro-active species, inhibitor adsorption, porous layer formation, etc., j is an imaginary number ($j^2 = -1$), ω is the angular frequency ($\omega = 2\pi f$) and the exponent n has values between −1 and 1. A value of −1 is a characteristic for an inductance, a value 1 corresponds to a resistor, and a value of 0.5 can be assigned to diffusion phenomenon [47].

3.4. Synergistic inhibition effect of Fe–NPC

The synergistic inhibition effect of inhibitors takes place when the total action of compounds is higher than the sum of each one individually. The synergism parameters (S) were calculated and listed in Table 3, using the following equation [48]:

$$S = \frac{1-(\eta_1+\eta_2)}{1-\eta_{1+2}} \quad (7)$$

where η_1 is the inhibition efficiency of purine derivatives (PU1 or PU2), η_2 is the inhibition efficiency of the Fe–NPC and η_{1+2} is the inhibition efficiency of Fe–NPC + purine inhibitor (PU1 or PU2) mixture.

It was found that the inhibition efficiency for solutions with Fe–NPC exhibit higher values compared to solutions without Fe–NPC, This reflects that Fe–NPC has a synergistic inhibitive effect with purine inhibitor on the carbon steel corrosion in sulfuric acid solution.

Generally, the values of S > 1 indicate a synergistic effect [49]. It is noticed that all values of S were greater than unity. This may suggest that the enhanced inhibition efficiency caused by the addition of Fe–NPC particles to the purine derivatives inhibitors was only due to synergistic effect.

3.6. Explanation for inhibition

The inhibition effect of investigated purine inhibitors in H_2SO_4 solution can be explained as follows; purine inhibitor might be protonated in the acid solution as following:

$$Inh + xH^+ \leftrightarrow [InhH_x]^{x+} \quad (8)$$

Thus, in aqueous acidic solutions, the inhibitor exists either as; (1) neutral molecules or (2) in the form of cations (protonated inhibitor). Generally, two modes of adsorption could be considered. The neutral inhibitor may be adsorbed on the metal surface via the adsorption mechanism, involving the displacement of water molecules from the metal surface and the sharing electrons between the heteroatom's and iron surface. The inhibitor molecules can be also adsorbed on the metal surface on the basis of donor–acceptor interactions between π-electrons of the heterocyclic and vacant d-orbitals of iron surface.

In another hand, SO_4^{-2} could adsorb on the metal surface, and then the protonated inhibitor may adsorb through electrostatic interactions between the positively charged inhibitor and already adsorbed sulfate ions [50]. It should be noted that the molecular structure of protonated inhibitor remains unchanged with respect to its neutral form, the heteroatoms on the ring remaining strongly blocked, so when protonated purine inhibitor adsorbed on the metal surface, co-ordinate bond may be formed by partial transference of electrons from the polar heteroatom's to the metal surface.

The inhibiting role of biosynthesis iron nanoparticles colloids (Fe–NPC) in mixture with purine inhibitors was explained by the formation of insoluble complex precipitate on the cathodic sites of the metal surface in neutral solution [51–54]. This reflects itself in a high adsorbability of the complexed purine derivatives (ligand). This phenomenon is consistent with results obtained for other inhibitor [55].

It was shown from Table 3 that the protection efficiency increases due to synergistic effects between Fe–NPC ions and purine derivatives. It is attributed to the formation and deposition of a protective purine derivatives/Fe–NPC complex on the carbon steel surface that inhibits the cathodic partial reaction [56, 57].

Table 3: Synergism parameters of carbon steel in 0.5 mol dm^{-3} H_2SO_4 solution at 298 K

Inhibitor	*C* (Purine) (mol dm^{-3})	*C* (Fe–NPC) (mol dm^{-3})	Tafel		EIS	
			η_p (%)	*S*	η_i (%)	*S*
PU1	5×10^{-3}	–	90.4	–	89.3	–
PU2	5×10^{-3}	–	95.1	–	93.0	–
Fe–NPC	–	1×10^{-3}	82.1	–	82.9	–
PU1+ Fe–NPC	1×10^{-4}	1×10^{-4}	95.3	1.82	92.9	1.84
PU2 + Fe–NPC	1×10^{-4}	1×10^{-4}	97.8	1.82	95.7	1.85

This supposed inhibition mechanism in presence of Fe–NPC and purine derivatives mixture is very clear in the potentiodynamic polarization measurement (Fig. 3), which the complex formation and deposition of purine derivatives/ Fe–NPC ions on the carbon steel surface leads to shift of corrosion potential (E_{corr}) to more negative (cathodic) direction, and hence consider cathodic inhibitors.

4. Conclusions

We succeed to biosynthesized Fe nanometal with Fusarium oxysporum fungus, the obtained material formed in nanoscale and had the mean particle size of 91 nm, which were confirmed by DLS and UV- absorption. This material improves the inhibition efficiency for PU1 and PU2, consequently act as a good inhibitor for the corrosion of carbon steel in (0.5 mol dm^{-3}) H_2SO_4. In our presented work, the potentiodynamic polarization curves indicated that PU1 and PU2 behave as mixed-type inhibitor, while the nanocomposite from (Fe–NPC) with PU1 and PU2 behave as cathodic inhibitor. EIS results indicate that the C_{dl} decrease when the inhibitors are added; this due to adsorption of these inhibitors on the steel surface. Which meaning the prepared nanocomposite have a synergism inhibitors, and the values of synergism parameter (*S*) are higher than unity.

Acknowledgement

The authors are greatly thankful to Egyptian Petroleum Research Institute (EPRI) fund and support.

References

[1] Obot, I. B.; Obi-Egbedi, N. O.; Umoren, S. A. The Synergistic Inhibitive Effect and Some Quantum Chemical Parameters of 2, 3-Diaminonaphtalene and Iodide Ions on The Hydrochloric Acid Corrosion of Aluminum. Corros. Sci. 2009, 51, 276–282.
[2] Azim, A.; Davood, Z.; Ali, F.; Mohammad, R. M.; Dariush, N.; Shahram, T.; Majid, M.; asim,B. Synthesis and Characterization of Gold Nanoparticles by Tryptophane. Am. J. Appl. Sci. 2009, 6, 691– 695.
[3] Tapan, K. S.; Andrey, L. R. Nonspherical Noble Metal Nanoparticles: Colloid Chemical Synthesis and Morphology Control. Adv. Mater. 2009, 21, 1–24.
[4] Simkiss, K.; Wilbur, K. M.; Biomineralization. Academic, New York, 1989.
[5] Mann, S.; Biomimetic Materials Chemistry. Wiley-VCH, New York, 1996.
[6] Sastry, M.; Ahmad A.; Khan I.; Kumar R. B. Biosynthesis of Metal Nanoparticles Using Fungi and Actinomycete. Current Science India 85. 2003, 2, 162 - 170.
[7] Ahmad, A.; Mukherjee, P.; Senapati, S.; Mandal, D.; Islam, Khan M.; Kumar, R.; Sastry, M.; Extracellular Biosynthesis Of Silver Nanoparticles Using The Fungus Fusarium Oxysporum. Colloids and surfaces B. 2003, 28, 313.
[8] Mukherjee, P.; Senapati, S.; Mandal, D.; Ahmad, A.; Khan, M. I.; Kumar, R.; Sastry, M. Extracellular Synthesis of Gold Nanoparticles by the Fungus Fusarium oxysporum. Chem. Biochem. 2002, 3, 461- 463.
[9] Senapati, S.; Mandal, D.; Ahmad, A.; Khan, MI.; Sastry, M.; Kuma,r R. Fungus Mediated
[10] Synthesis of Silver Nanoparticles: a Novel Biological Approach. Ind. J. Phys. 2004, 78A, 101–105.
[11] Bansal, V.; Rautaray, D.; Bharde, A.; Ahire, K.; Sanyal, A.; Ahmad, A. Fungus-Mediated Biosynthesis of Silica And Titania Particles. J. Mater. Chem. 2005, 15, 2583 - 2589.
Bansal, V.; Poddar, P.; Ahmad, A.; Sastry, M. Room-Temperature Biosynthesis of Ferroelectric Barium Titanate Nanoparticles. Am. Chem. Soc. 2006, 128, 11958 - 11963.
[12] Riddin, TL.; Gericke, M.; Whiteley, C. G. Analysis of the Inter- and Extracellular Formation of Platinum Nanoparticles by Fusarium Oxysporum f. sp. lycopersici Using Response Surface Methodology. Nanotech. 2006, 17, 3482.
[13] Kumar, S. A.; Ayoobul, A. A.; Absar, A.; Khan, MI. Extracellular Biosynthesis of CdSe Quantum Dots by the Fungus, Fusarium Oxysporum. J. Biomed. Nanotech. 2007, 3, 190 - 194.
[14] Uddin, I.; Adyanthaya, S.; Syed, A.; Selvaraj, K.; Ahmad, A.; Poddar, P. Structure and Microbial Synthesis of Sub-10 nm Bi2O3 Nanocrystals. J. Nanosci. Nanotech. 2008, 8, 3909.
[15] Badr, G. E. The Role of Some Thiosemicarbazide Derivatives as Corrosion Inhibitors for C-Steel in Acidic Media. Corro. Sci. 2009, 51, 2529–2536.
[16] Hana, C.; Yon, K. S.; Kyoo, Y. K.; Jong M. P. Encapsulation of Triethanolamine as Organic Corrosion Inhibitor Into Nanoparticles and Its Active Corrosion Protection for Steel Sheets. Surf. Coat. Technol. 2012, 206, 2354–2362.
[17] Behpour, M.; Ghoreishi, S. M.; Khayatkashani, M.; Soltani, N. Green Approach to Corrosion Inhibition of Mild Steel in Two Acidic Solutions by The Extract of Punicagranatum Peel and Main Constituents. Mater. Chem. Phys. 2012, 131, 621–633.
[18] Palomar-Pardavé, M.; Romero-Romo, M.; Herrera-Hernández, H.; Abreu-Quijano, M. A. Likhanova, N. V.; Uruchurtu, J.; Juárez-García, J. M. Influence of the Alkyl Chain Length of 2 Amino 5 Alkyl 1,3,4 Thiadiazole Compounds on the Corrosion Inhibition of Steel Immersed in Sulfuric Acid Solutions. Corros. Sci. 2012, 54, 231–243.
[19] Deng, S.; Li, X. Inhibition by Ginkgo leaves Extract of the Corrosion of Steel in HCl and H2SO4 Solutions. Corros. Sci. 2012, 55, 407–415.
[20] Mohamed, H. A.; Farag, A. A.; Badran, B. M. Friendly to Environment Heterocyclic Adducts as Corrosion Inhibitors for Steel in Water-Borne Paints. J. Appl. Polym. Sci. 2010, 117, 1270-1278.
[21] Li, X.; Deng, S.; Fu, H. Mu, G. Inhibition Effect of 6-Benzylaminopurine on the Corrosion of Cold Rolled Steel in H2SO4 Solution. Corros. Sci. 2009, 51, 620–634.
[22] Yan, Y.; Li,W. H.; Cai, L. K.; Hou, B. R. Electrochemical and Quantum Chemical Study of Purines as Corrosion Inhibitors for Mild Steel in 1 M HCl Solution. Electrochim. Acta. 2008, 53, 5953-5960.
[23] Solmaz, R. Investigation of Corrosion Inhibition Mechanism and Stability of Vitamin B1 on Mild Steel in 0.5 M HCl Solution. Corros. Sci. 2014, 81, 75-84.
[24] Moteshafi, H.; Mousavi, S. M.; Shojaosadati, S. A.; The Possible Mechanisms Involved in Nanoparticles Biosynthesis. J. Indus. Engin. Chem. 2012, 18, 2046–2050.
[25] Eftink, M. R.; Ghiron, C. A. Frequency Domain Measurements of the Fluorescence Lifetime of Ribonuclease T1. Biochem. 1987, 52, 467- 473.
Farag, A. A.; Noor El-Din, M. R.; The Adsorption and Corrosion Inhibition of Some Nonionic Surfactants on API X 65 Steel Surfaces in Hydrochloric Acid. Corros. Sci. 2012, 64, 174–183.
[26] Riggs, O. L. Jr.; Nathan, C. C. Corrosion Inhibitors, second ed., NACE (National Association of Corrosion Engineers), Houston, TX, 1973.
[27] Quraishi, M. A.; Jamal, D. Dianils as New and Effective Corrosion Inhibitors for Mild Steel in Acidic Solutions. Mater. Chem. Phys. 2003, 78, 608-613.
[28] Ghanbari, A.; Attar, M. M.; Mahdavian, M. Corrosion Inhibition Performance of Three Imidazole Derivatives on Mild Steel in 1 M Phosphoric Acid. Mater. Chem. Phys. 2010, 124, 1205-1209.
[29] Oguzie, E. E.; Li, Y.; Wang, F. H. Corrosion Inhibition and Adsorption Behavior of Methionine on Mild Steel in Sulfuric Acid and Synergistic Effect of Iodide Ion. Corros. Sci. 2007, 310, 90–98.
[30] Lagrenée, M.; Mernari, B.; Bouanis, M.; Traisnel, M.; Bentiss, F. Study of the Mechanism and Inhibiting Efficiency of 3,5-bis(4-Metylthiophenyl)-4H-1,2,4-Triazole on Mild Steel Corrosion in Acidic Media. Corros. Sci. 2002, 44, 573–588.
[31] Singh, A. K.; Quraishi, M.A. Effect of Cafazolin on the Corrosion of Mild Steel in HCl Solution. Corros. Sci. 2010, 52, 152–160.
[32] Labjar, N.; Lebrini, M.; Bentiss, F.; Chihib, N. E.; El Hajjaji, S.; Jama, C. Corrosion Inhibition of Carbon Steel and Antibacterial Properties of Aminotris-(Methylnephosnic) Acid. Mater. Chem. Phys. 2010, 119, 330–336.
[33] Migahed, M. A.; Farag, A. A.; Elsaed, S. M.; Kamal, R.; Mostfa, M.; Abd El-Bary, H. Synthesis of a New Family of Schiff Base Nonionic Surfactants and Evaluation of their Corrosion Inhibition Effect on X-65 Type Tubing Steel in Deep Oil Wells Formation Water. Mater. Chem. Phys. 2011, 125, 125–135.
[34] Al-Sabagh, A. M.; Nasser, N. M.; Farag, A. A.; Migahed, M. A.; Eissa, A. M. F.; Mahmoud, T. Structure Effect of Some Amine Derivatives on Corrosion Inhibition Efficiency for Carbon Steel in Acidic Media Using Electrochemical and Quantum Theory Methods. Egyp. J. P. 2013, 22, 101–116.
[35] Abdel-Gaber, A. M.; Masoud, M. S.; Khalil, E. A.; Shehata, E. E. Electrochemical Study on the Effect of SCHIFF Base and its Cobalt Complex on the Acid Corrosion of Steel. Corros. Sci. 2009, 51, 3021–3024.
[36] Migahed, M. A.; Farag, A. A.; Elsaed, S. M.; Kamal, R.; El-Bary, H. A. Corrosion Inhibition of Steel Pipelines in Oil

Well Formation Water by a New Family of Nonionic Surfactants. Chem. Eng. Commun. 2012, 199, 1335-1356.
[37] Farag, A. A.; Hegazy, M. A. Synergistic Inhibition Effect of Potassium Iodide and Novel Schiff
[38] Bases on X65 Steel Corrosion in 0.5 M H2SO4. Corros. Sci. 2013, 74, 168–177.
[39] Musa, A. Y.; Jalgham, R. T.T.; Abu Bakar, M. Molecular Dynamic and Quantum Chemical Calculations for Phthalazine Derivatives as Corrosion Inhibitors of Mild Steel in 1 M HCl. Corros. Sci. 2012, 56, 176–183.
[40] Khaled, K. F.; Hackerman, N. Investigation of the Inhibitive Effect of Ortho-Substituted Anilines on Corrosion of Iron in 1 M HCl Solutions. Electrochim. Acta 2003, 48, 2715-2723.
[41] Heydari, M.; Javidi, M. Corrosion Inhibition and Adsorption Behaviour of an Amido-Imidazoline Derivative on API 5L X52 Steel in CO2-Saturated Solution and Synergistic Effect of Iodide Ions. Corros. Sci. 2012, 61, 148–155.
[42] Kissi, M.; Bouklah, M. Hammouti, B. Benkaddour, M. Establishment of Equivalent Circuits from Electrochemical Impedance Spectroscopy Study of Corrosion Inhibition of Steel by Pyrazine in Sulphuric Acidic Solution. Appl. Surf. Sci. 2006, 252, 4190- 4197.
[43] Larabi, L.; Harek, Y.; Benali, O.; Ghalem, S. Hydrazide Derivatives as Corrosion Inhibitors for Mild Steel in 1 M HCl. Prog. Org. Coat. 2005, 54, 256-262.
[44] Popova, A.; Sokolova, E.; Raicheva, S.; Christov, M. AC and DC Study of the Temperature Effect on Mild Steel Corrosion in Acid Media in the Presence of Benzimidazole Derivatives. Corros. Sci. 2003, 45, 33-58.
[45] Keles, H.; Keles, M.; Dehri, I.; Serindag, O. The Inhibitive Effect of 6-Amino-m-Cresol and its Schiff Base on the Corrosion of Mild Steel in 0.5 M HCI Medium. Mater. Chem. Phys. 2008, 112, 173–179.
[46] Priya, A. R. S.; Muralidharam, V. S.; Subramania, A. Development of Novel Acidizing Inhibitors for Carbon Steel Corrosion in 15% Boiling Hydrochloric Acid.Corro.2008, 64, 541–552.
[47] Bommersbach, P.; Alemany-Dumont, C.; Millet, J. P.; Normand, B. Hydrody-namic Effect on the Behaviour of a Corrosion Inhibitor film: Characterization by Electrochemical Impedance Spectroscopy. Electrochimica Acta 2006, 51, 4011–4018.
[48] Larabi, L.; Harek, Y.; Traisnel, M.; Mansri, A. Synergistic Influence of Poly (4-vinylpyridine) and Potassium Iodide on Inhibition of Corrosion of Mild Steel in 1 M HCl. J. Appl. Electrochem. 2004, 34, 833–839.
[49] Musa, A. Y.; Abu Bakar, M.; Kadhum, A. H.; Takriff, M. S.; Tien, L. T.; Synergistic Effect of Potassium Iodide with Phthalazone on the Corrosion Inhibition of Mild Steel in 1.0 M HCl. Corros. Sci. 2011, 53, 3672–3677.
[50] Bentiss, F.; Traisnel, M.; Lagrenée, M. The substituted 1,3,4-oxadiazoles: a new class of corrosion inhibitors of mild steel in acidic media, Corros. Sci. 2000, 42, 127–146.
[51] Rajendran, S.; Apparao, B. V.; Palaniswamy, N. Synergistic And Antagonistic Effects Existing Among Polyacrylamide, Phenyl Phosphonate And Zn2+ On The Inhibition Of Corrosion Of Mild Steel In A Neutral Aqueous Environment. Electrochim. Acta 1998, 44, 533–553.
Rajendran, S.; Reenkala, S. M.; Anthony, N.; Ramaraj, R. Synergistic Corrosion Inhibition By The Sodium Dodecylsulphate–Zn2+ System. Corros. Sci. 2002, 44, 2243–2252.
Amar, H.; Benzakour, J.; Derja, A.; Villemin, D.; Moreau, B.; Braisaz, T.; Tounsi, A. Synergistic Corrosion Inhibition Study Of Armco Iron In Sodium Chloride By Piperidin-1-Yl-Phosphonic Acid–Zn2+ System. Corros. Sci. 2008, 50, 124–130.
Cotton, F. A.; Wilkenson, G. Advanced Inorganic Chemistry, 4th ed., Wiley, New York, 1980, pp. 81, 119, 121.
[52] Wahdan, M. H. The Synergistic Inhibition Effect and Thermodynamic Properties of 2-Mercaptobenzimidazol and Some Selected Cations as a Mixed Inhibitor for Pickling of Mild Steel in Acid Solution. Mater. Chem. Phys. 1997, 49, 135–140.
[53] Sayed, S. Y.; El-Deab, M. S.; El-Anadouli, B. E.; Ateya, B. G. Synergistic Effects of Benzotriazole and Copper Ions on the Electrochemical Impedance Spectroscopy and Corrosion Behavior of Iron in Sulfuric Acid. J. Phys. Chem. B 2003, 107, 5575- 5585.
[54] Ismail, K. M. Evaluation of Cysteine as Environmentally Friendly Corrosion Inhibitor for Copper in Neutral and Acidic Chloride Solutions. Electrochimia Acta 2007, 52, 7811–7819.

Author Profile

Ibrahim Mohamed Nassar, PhD in Physical Chemistry Kazan state technological University (KSTU), Institute of Polymer, Faculty of Rubber & Elastomer Technology and processing. Postdoctoral in Physical Chemistry National Academy of Sciences Institute of Physics.